OPEN

How micron-sized dust particles determine the chemistry of our Universe

François Dulieu[1], Emanuele Congiu[1], Jennifer Noble[2], Saoud Baouche[1], Henda Chaabouni[1], Audrey Moudens[1], Marco Minissale[1] & Stéphanie Cazaux[3]

[1]LERMA Université de Cergy-Pontoise, Observatoire de Paris, ENS, UPMC 8112 du CNRS, 5 mail Gay Lussac, 95000 Cergy Pontoise Cedex, France, [2]Aix-Marseille Université, PIIM UMR 7345, 13397, Marseille, France, [3]Kapteyn Astronomical Institute, PO box 800, 9700AV Groningen, The Netherlands.

In the environments where stars and planets form, about one percent of the mass is in the form of micro-meter sized particles known as dust. However small and insignificant these dust grains may seem, they are responsible for the production of the simplest (H_2) to the most complex (amino-acids) molecules observed in our Universe. Dust particles are recognized as powerful nano-factories that produce chemical species. However, the mechanism that converts species on dust to gas species remains elusive. Here we report experimental evidence that species forming on interstellar dust analogs can be directly released into the gas. This process, entitled chemical desorption (fig. 1), can dominate over the chemistry due to the gas phase by more than ten orders of magnitude. It also determines which species remain on the surface and are available to participate in the subsequent complex chemistry that forms the molecules necessary for the emergence of life.

ighty years ago, dust was first identified in the interstellar space as the "something" which is obscuring the light coming from stars[1]. For several decades, dust grains were thought to be only passive and annoying entities present towards any astrophysical objects that astronomers wanted to observe. Only in the 60 s, the real nature of dust was revealed and it appeared that dust is a powerful interstellar catalyst[2]. The presence of several chemical species that cannot form efficiently in the gas only highlighted the need to explore the chemistry occurring on interstellar dust. At first, the use of chemistry occurring on dust to palliate the failure of gas phase chemistry was qualified as the refuge of the scoundrels[3]. However, while the role of dust as interstellar catalyst is now well recognized, the mechanism that allows the formed species on the surface to populate the gas phase is still unknown. This is a real paradox and issue of modern astrochemistry: to reconcile almost non-observable solid phase dust catalysis to observable products in the gas phase. Observations of deeply embedded protostars show that the disappearance of CO in the gas (because CO sticks on the dust) leads to a high abundance of CH_3OH in the gas[4]. This anti-corelation demonstrates that CO converts into CH_3OH on dust and is released into the gas phase through an efficient mechanism. It appears that many reactions occurring on dust grains are accompanied with an excess energy which is too large to dissipate. Consequently, the formed species are ejected in the gas phase upon formation. This process, called chemical desorption, implies that the chemistry occurring on interstellar dust affects the composition of the gas. Whereas the existence of this process, first suggested one decade ago[5], has been shown theoretically[6–10], it has been experimentally observed only for H_2 molecules[11–14] which is the most favorable expected case (very light, weakly bounded, very exothermic). In this work, we present the first experimental evidence of this process for several reactions occurring on dust analogs. We show that chemical desorption is very important (more than 90% of water formed through OH + H on the dust is released in the gas phase) and has been considerably underestimated by previous assumptions. We discuss the importance of this mechanism in comparison with the chemistry in the gas, and show that it can dramatically change the chemical composition of the interstellar medium. In this sense, because the chemical composition of a medium is one of the main observational tool used to determine physical conditions, we show that current astrochemical models have to account for the catalytic role of dust due to chemical desorption in order to properly describe/predict observations. This new result also affects our current understanding of star formation. By changing the abundances of molecules present in the gas of a cloud that undergoes gravitational collapse to form a star, the gas cools more or less rapidly, which impacts the efficiency and characteristics (mass, binarity) of star formation.
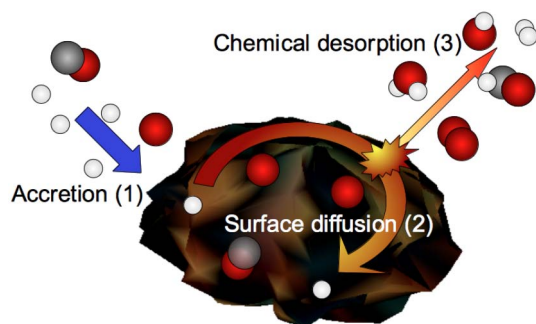
Figure 1 | Sketch that illustrates the chemical desorption process. Species coming from the gas accrete on the dust surface and can meet each other to form other species. For some reactions shown in this study, the formed product is ejected in the gas.

Results

We study experimentally the formation of water on silicate surfaces. For this purpose, we deposit O_2 molecules on silicates, and deposit D atoms in a second step. The surface chosen in this study is usually used as interstellar dust analogs. After deposition at 10 K, the surface temperature is increased up to 200 K and molecules are measured in the gas with a mass spectrometer. The results of these experiments are presented in fig. 2. The solid lines represent the thermal desorption spectra of O_2 (mass 32), the dashed lines the signal for D_2O (mass 20), while dotted lines the signal of D_2O_2 (mass 36), as the temperature of the surface is increased at 0.04 K/s. The thermal desorption spectra of the 3 different species on silicate surfaces are represented in red. For comparison, we also report our experimental results for the formation of water on graphite (green), and non porous ice (blue).

The black line represents the thermal desorption spectrum when only O_2 is deposited on silicate surfaces. It desorbs as a single peak at around 35 K and the integrated signal corresponds to 1.0 monolayer (1 ML $\sim 10^{15}$ atoms/cm²). The red lines (solid for O_2, dashed for D_2O and dotted for D_2O_2) represent the thermal desorption spectra when O_2 is similarly deposited, and is exposed to 4 10^{15} atoms/cm² of

D. In this case, the desorption of O_2 around 35 K is very weak compared to the deposition of O_2 only, meaning than most ($\geq 90\%$) of the initial O_2 molecules have disappeared. D_2O and D_2O_2 desorption features are observed at 150 K, and before 200 K, respectively. The location of these peaks in temperature allow to derive the binding energies of the different species on the substrate. These binding energies are reported in table 1. Previous studies showed that O_2 reacts quickly with D, forming O_2D, D_2O_2 and finally D_2O[16–18]. The area of the desorbed peaks indicates that only 35% of the oxygen has been included in the D_2O and D_2O_2 molecules, meaning than around 65% of the O_2 molecules are missing from the surface.

The O_2 molecules missing in the desorption spectra are believed to be ejected into the gas phase during exposure with D atoms, following chemical reaction. In this sense, once new species are formed, and are unable to thermalize on the surface, they are released into the gas phase (the so called chemical desorption). To prove the existence of this process, we monitor the mass signal during D irradiation, with the quadrupole mass spectrometer placed in a position remote from the sample. The measurements are reported in the inset of fig. 2 before and during D irradiation for D_2O (mass 20), DO_2 (mass 34) and D_2O_2 (mass 36). We observe a direct D_2O signal far above the

Table 1 | TPD desorption peaks and associated binding energies of the molecules on the silicate surface

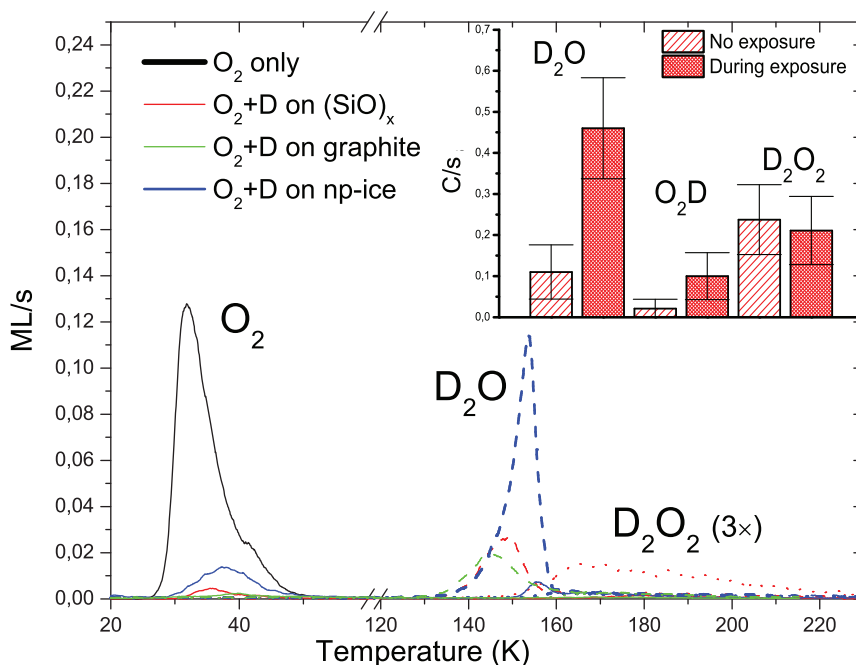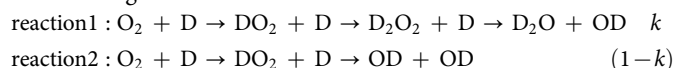| Species	TPD peak	Binding energy (K)	ref.
H_2	12 K	300	[11]
H		500	[20]
O		1100	This work
O_2	40 K	1255	[15]
O_3	67 K	2100	Minisale et al. submitted
O_2H		4000	
OH	140 K	4600	
H_2O	145 K	4800	This work and [21,22]
H_2O_2	180 K	6000	This work

Figure 2 | Experimental evidence of chemical desorption. Desorption peaks of O_2 (solid), D_2O (dashed) and D_2O_2 (dotted) species after the exposure of D atoms on 1 ML coverage of O_2 ice deposited on different substrates (silicates SiOx in red, graphite in green and np-ASW ice in blue) held at 10 K. Inset: D_2O, D_2O_2 and D_2O monitored with the QMS during the exposure of D atoms on 1 ML coverage of O_2 ice deposited on the silicate substrate at 10 K.

noise level, indicating that D_2O is chemically desorbed. On the other hand, we do detect a very small increase of the DO_2 signal (in the noise) but no increase of the D_2O_2 signal. OD (mass 18) and O_2 (mass 32) are also monitored, but the presence of H_2O (mass 18) and O_2 as minor contaminants in the vacuum decreases the signal to noise ratio, allowing only a one sigma detection of O_2. The measurement before/during irradiation provides clear evidence of the chemical desorption, and that the product concerns mainly D_2O. The signal before and during irradiation cannot be directly compared since the QMS is not located at the same place during these experiments. For the TPDs, it is placed in front of the sample to maximize the signal. In the irradiation configuration, it is placed closed to the surface, but with an angle of about 45°.

Our experimental results show that in the case of water formation on a silicate substrate, 65% of the O_2 molecules initially on the substrate are no longer present after D irradiation. By measuring the amount of species desorbing before/during the irradiation of O_2 with D atoms, we show that repetitive addition of D to O_2 leads to the detection of D_2O in the gas phase. The possible reactions routes are the following:

$$\text{reaction1}: O_2 + D \rightarrow DO_2 + D \rightarrow D_2O_2 + D \rightarrow D_2O + OD \quad k$$
$$\text{reaction2}: O_2 + D \rightarrow DO_2 + D \rightarrow OD + OD \quad\quad (1-k)$$

The branching ratio of these two reactions are k and $(1 - k)$. The table 2 reports the reactions involved in our experiment as well as their exothermicities. The reaction $O_2 + D$ leading to DO_2 is slightly exothermic (2.3 eV) but we only see a slight increase of the mass signal (mass 34) when O_2 is exposed to D atoms (this signal is in the noise). The reaction $DO_2 + D$ leading to D_2O_2 has an exothermicity of 3.7 eV, but D_2O_2 is not detected in the gas phase during irradiation. Previous studies showed that H_2O_2 (D_2O_2) can easily decompose in H_2O (D_2O) on the wall of chamber[19], meaning that the H_2O (D_2O) signal obtained is due to molecules bouncing on the wall. In our experimental configuration, the number of bounced molecules that are detected are less than 10% (see Ref. 13), and can be neglected in our analysis. We know that D_2O_2 leaving in the gas phase cracks into D_2O (for ~40%) but that ~60% stays under the form of D_2O_2. The cracking pattern of D_2O_2 is estimated during the TPD after 160 K, where we see a signal at the masses 20 (D_2O) and 36 (D_2O_2) simultaneously. Therefore, if D_2O_2 is chemically desorbed into the gas phase, we should see an increased of the signal during irradiation. The reaction $DO_2 + D$ can also lead to $OD + OD$, and has an exothermicity of 1.6 eV. However, we are not able to detect OD molecules since their mass coincide with H_2O (mass 18) which is contaminating the mass spectra. We are therefore not able to derive the fraction that is chemically desorbed for this reaction. The reaction $D_2O_2 + D \rightarrow D_2O + OD$ is exothermic with an energy of 3.1 eV, and the reaction $OD + D \rightarrow D_2O$ has an exothermicity of 5.2 eV. Since D_2O is observed in the gas phase during exposition of O_2 with D atoms, we can not differentiate which of these two routes is responsible for the important chemical desorption of D_2O which is observed.

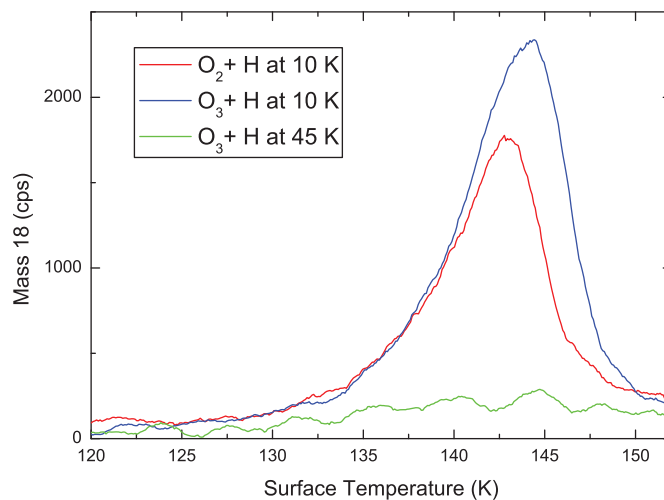
Figure 3 | Desorption spectra of water after its formation via 1 ML of O_2 followed by 7 10^{15} H/cm² on silicates held at 10 K (blue); 1 ML of O_3 followed by 7 10^{15} H/cm² atoms on a surface held at 10 K (red) and at 45 K (green).

We perform complementary TPD experiments to address the origin of the very important chemical desorption of D_2O. Here we use hydrogen instead of deuterium. Figure 3 represents the desorption spectra of water after its formation via 10^{15} atoms/cm² of O_2 followed by 7 × 10^{15} atoms/cm² of H atoms on a surface held at 10 K (blue); 10^{15} atoms/cm² of O_3 followed by 7 × 10^{15} atoms/cm² of H atoms on a surface held at 10 K (red) and 45 K (green). We can see that in the case of O_3, there is a lower production of H_2O, because the formation of water is made of two sub-routes $O_3 + H \rightarrow OH + O_2$. Performing experiments at 45 K, where O_2 is evaporating at a high rate, almost forbid the $O_2 + H$ sub-route, so the $O_3 + H$ at 45 K is almost like observing the $OH + H$ reaction. We can see clearly that there is almost no water produced that way, indicating a very strong chemical desorption during exposure through the reaction $OH + H$. To check that the disappearance of the water signal for $O_3 + H$ at 45 K is not due to the fact that the reaction does not proceeds, we measure the amount of O_3 present on the surface as O_3 is exposed to H atoms. We see that the peak of O_3, located at 67 K in the TPD, decreases as the exposure with H atoms increases. This shows that even if the residence time of H atoms on the surface is short at 45 K, it is long enough to proceed radical-radical reactions, as observed here for the reaction $O_3 + H$ and also observed for $NO + H$[23]. To summarize, we show that the $OH + H$ route is the one responsible for the important amount of water during exposure of O_2 with H or D. Since most of the water formed through this route is ejected in the gas phase, this allows us to bring further constrains on our first TPD experiment. The reaction $O_2 + D$ leads to the formation of D_2O_2 and then $D_2O + OD$, or to the formation of 2 OD. Since OD on the surface reacts with a D to form D_2O and is ejected in the gas, D_2O and D_2O_2 observed in the TPD are the results of the reaction 1. This implies that the 35% of O_2 found on the surface come from the reaction 1, and that the branching ratio is $k = 0.35$. The reactions occurring in our experiment, as well we the fraction of species chemically desorbed are reported in table 2.

Similar experiments have been performed on graphitic surface and on water ice substrate (Dulieu et al. in prep). For graphite, 80% of the O_2 molecules initially on the substrate are no longer present after D exposure. For the water ice as a substrate, this percentage strongly depends on the morphology of the ice, and can vary from almost 0% in the case of porous ice, to 40% in the case of non porous amorphous ice. These percentages are the fraction of the newly formed species that are ejected into the gas phase upon formation due to the high

Table 2	Chemical desorption efficiency of different reactions		
Reaction	Exothermicity (eV)	Fraction released in gas phase
$OD + D \rightarrow D_2O$	5.2	>90%
$O_2 + D \rightarrow DO_2$	2.3	<10%
$DO_2 + D \rightarrow D_2O_2$	3.7	<10%
$DO_2 + D \rightarrow OD + OD$	1.6	
$D_2O_2 + D \rightarrow D_2O + OD$	3.1	<10%
$O + O \rightarrow O_2$	5.2	60% Dulieu et al. in prep.
$O + O_2 \rightarrow O_3$	1.1	≤10% Minissale et al. in prep.

exothermicity of the reaction. Coupling to the substrate (phonons) is believed to be the source of the different rates observed for different substrates. Therefore, our results show (table 2) that the fraction of species released into the gas phase upon formation do not depend directly on the exothermicity of the reaction and on the binding energy of the products. The mass of the formed species also plays a fundamental role, as well as the type of substrate that is considered. Many follow-up experimental studies using different reactions/substrates are envisaged to understand the nature of the chemical desorption process.

Discussion

To estimate the impact of chemical desorption on the gas phase composition of astrophysical environments, we use a theoretical model[10,24], but include the chemical desorption yields derived from the experiments presented in the previous section. In this sense, we quantify the direct impact of the chemistry on dust on the gas phase. For some reactions occurring on the surface, an important amount of the formed species are ejected in the gas phase. Therefore, within the parameter range at which these reactions dominate the chemistry on the dust surface, an important contribution in the gas phase is expected. Figure 4 illustrates the chemical desorption of H_2O, OH and O_2 as a function of the dust temperature. The calculations of these efficiencies are reported in the methods section. These efficiencies are the amount of O that is converted to OH, H_2O and O_2 on the dust and directly released into the gas phase. In this sense, the calculated efficiencies directly provide the conversion rate of gas phase atomic oxygen into another gas phase species by the use of grain surface chemistry. As OH is formed through O + H, O_2 through O + O, or water through OH + H, an important fraction of the newly formed molecules is released into the gas phase. The formation efficiency is on the order of ~30% for OH (below 15 K) and ~70% for water (below ~25 K). For O_2, there are two main temperature ranges where desorption into the gas phase is important. The first one, located around 17 K, has an efficiency of about 4%, while the second one, located around ~35 K, has an efficiency of 0.2%. If a strong UV field is considered in our calculations, then the species on the surface can be photo-dissociated and reform. We consider a strong radiation filed ($G_0 = 100$, which corresponds to 100 times the ambient UV radiation field), and show that the efficiency of O_2 formation is increased by a factor of 5. On the other hand, the formation of OH and H_2O is unchanged.

It is now possible to describe analytically the formation rates of chemical species on dust with simple formulae usable for any astrochemical model. These rates $k_{OH,dust}$, $k_{H_2O,dust}$ and $k_{O2,dust}$ (in $cm^3 \ s^{-1}$) are reported in the supplementary material. The rate of the formation of species on dust (that are release in the gas) can be directly compared with gas phase rates in order to determine how molecules form in different environments with different physical conditions.

In the gas phase, the formation routes of water (OH + H_2) and OH (O + H_2) are associated with barriers of 1736 K, 3150 K, respectively[25]. While the gas phase formation rate of O_2 through OH + O, is still subject to debates (no barrier until T_{gas} ~150 K see references in[26]). The rates $k_{OH,gas}$, $k_{H_2O,gas}$ (in $cm^3 \ s^{-1}$) are reported in the supplementary material.

If we compare the formation rates of species via gas or dust routes, we need to compare $R_{gas} = n_X \cdot n_Y \cdot k_{gas}$ to $R_{dust} = n_X \cdot n_H \cdot k_{dust}$. In our case, X is oxygen, since we are dealing with the formation of oxygenated species.

The formation of OH (and water) on dust surfaces dominates by 12 (9) orders of magnitude the gas phase route for a gas at 100 K, while this becomes of 0 (2) for a gas at 500 K. These estimations are made considering the dust temperature in the range (0–15 K) for OH and (0–25 K) for water (and with the density of gas phase O and OH as $nOI = 10^{-4} \ n_H$, $nOH = 10^{-7} \ n_H$).

Searches of O_2 with ground based telescopes and space missions such as SWASS and ODIN indicated that O_2 has a widespread low abundance. O_2 remained unseen allowing to derive some upper limits ($X(O_2) \leq 10^{-7}$ [27,28]). However, while recent Hershel observations confirmed the general trend that O_2 has very low abundances (detection of O_2 towards ρOph, $X(O_2) \sim 10^{-8}$ [29]), one isolated high abundance of O_2 has been reported towards ORION[26]. This high abundance has been attributed to the presence of warm dust, or to shocks. In this work, our model shows an alternative efficient way to form O_2 in the gas phase through chemical desorption from dust. This efficiency is important only for very specific conditions (T_{dust} ~30–40 K and high UV field), which could explain why the detection of O_2 is seen only in isolated cases. This will be investigated in a forthcoming paper.
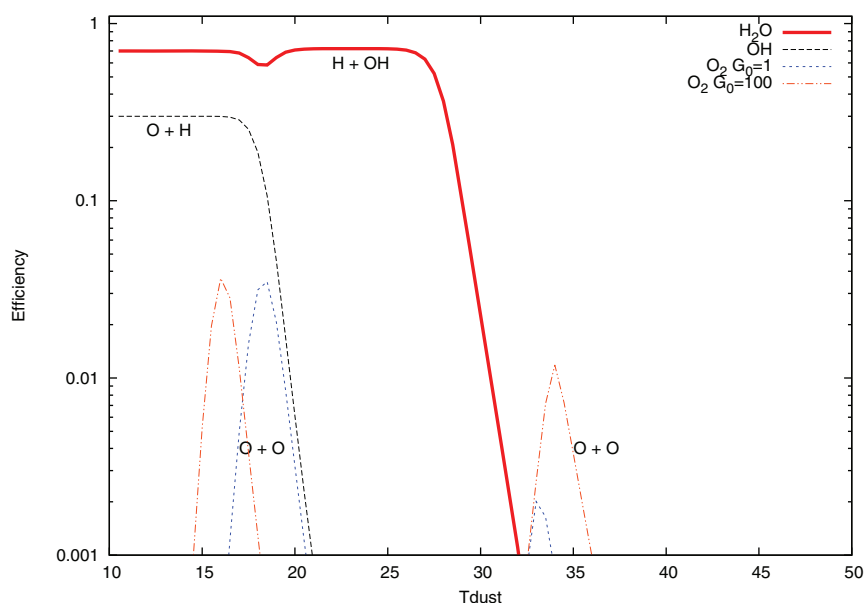

Figure 4 | Efficiency of chemical desorption as a function of dust temperature. This efficiency represents the fraction of oxygen released into the gas as OH, H_2O and O_2. The first three reactions are computed for a UV field of $G_0 = 1$, while the final three are for $G_0 = 100$. Note that the amount of O_2 released into the gas is significantly enhanced in the presence of a strong UV field.

In summary, we report the first experimental evidence that species which form on the surface of interstellar dust grains can subsequently be released into the gas phase due to the exothermicity of the reaction. By depositing O_2 molecules on several types of surfaces, and depositing D atoms in a second step, we show that an important fraction of the newly formed species are released into the gas phase during their formation, therefore confirming the existence and importance of the chemical desorption process. We also show that chemical desorption is sensitive to the type of surface upon which the formation reaction occurs. We derive canonical expressions for the formation of water, OH and O_2 in the gas phase due to chemical desorption. These expressions can be implemented in any astrophysical model to properly account for the chemistry occurring in space. We show that this process, that covers gas phase species to another though dust, dominates by many orders of magnitude gas phase chemistry in the typical astrophysical environments where water and water ice are forming.

The process highlighted in this study, chemical desorption, has an important impact on the chemistry and thermodynamics of our Universe. In regions where stars are forming, the presence of dust dramatically influences the gas phase composition, changing the abundances of molecules available to cool the gas. Therefore, a cloud that undergoes gravitational collapse to form a star will cool more or less rapidly, depending on the available coolants, and this impacts the efficiency and characteristics (mass, binarity) of star formation. In this sense, the existence of chemical desorption, illustrated in this study, not only impacts the chemical composition of our Universe, but affects the way stars form.

Methods

Experimental setup. Experiments were performed using the FORMOLISM set-up[13]. In an ultra high vacuum chamber, a gold mirror covered with amorphous silicate (or a graphite substrate) is held at 10 K. All the experiments are performed in the sub-monolayer regime (1 monolayer means that the surface is covered at 100%), to ensure that the interactions of the species with the surface is not perturbed by layering effects. The surface coverage is determined using the specific desorption properties of the second layer[15]. One layer (or less) of O_2 molecules is deposited at 10 K. Coincidently, or just after O_2 deposition, a D beam (with a dissociation efficiency of 70%) is aimed at the solid sample covered with O_2. In a second phase, the surface temperature is increased and the desorption flux is monitored using a movable quadrupole mass spectrometer, placed 3 mm away from the surface.

Microscopic model. To estimate the impact of chemical desorption on the gas phase composition of astrophysical environments, we use the chemical network presented in previous studies[10,24], but include the chemical desorption yields derived from the experiments presented in this work (Table 1). We solve this chemical network using the rate equations method. We follow the evolution of the species on the surface in monolayers, and calculate the amount of newly formed species that desorb into the gas phase due to chemical desorption.

The main processes that are necessary to describe the chemistry occurring on a grain surface are described in details in this section. Here we enumerate these different processes: (1) species from the gas accrete on the dust (2) species on the dust diffuse on the surface (3) species on the surface react to form a product that is released in the gas phase (illustrated in fig. 1 with probabilities listed in table 1) (4) same than 3 but the product stays on he surface (5) evaporation of the surface species into the gas phase (6) photo-dissociation of surface species by UV photon. Our rate equation model follows the evolution of surface species with time. For this, we take into account the different processes occurring to the different species and calculate their associated rates. These processes are the following:

1) Species from the gas phase accrete onto the dust with a rate:

$$R_{acc_X} = \frac{n_X v_X S}{n_{site}} \text{Monolayer s}^{-1},\qquad(1)$$

where n_X and v_X are, respectively, the gas phase density and velocity of the species X , n_{site} is the density of sites on the dust (10^{15} cm^{-2}), and S is the sticking coefficient of the species on the dust. We consider that S = 1, meaning that when a species arrives on the dust, it directly sticks to the surface.

2) Species present on the surface evaporate from the surface with a rate:

$$R_{evap(X)} = v_X \times \exp\left(-\frac{E_X}{k_B T}\right),\qquad(2)$$

where v_X is the oscillation factor of the species (which is 10^{12} s^{-1} on physisorbed sites), and E_X is the binding energy of species X, or in previous work[30].

3) Species on the surface can diffuse on the surface with a mobility:

$$\alpha_X = v_X \times \left(\exp\left(-0.4a\sqrt{m_X Ea_X}\right) + \exp\left(-\frac{Ea_X}{k_B T}\right)\right).\qquad(3)$$

The first exponential represents the diffusion occurring through tunneling, and the second through thermal hopping. Ea_X is the energy of the barrier between two physisorbed sites (which is considered here as 2/3 of the binding energies E_X), a the width of the barrier (in Å), and m_X the mass of the species X in amu. Note that the quantum tunneling is approximated[20]. Oxygen, even with its high mass, is observed to tunnel quite efficiently on the surface (Dulieu et al. submitted). We therefore adopt a barrier width of 1Å and barrier height of 500 K for the diffusion of oxygen on silicates. Oxygen can diffuse on the surface via quantum tunneling until $T_{dust} = 25$ K.

4) Species on the surface can be photodissociated by UV photons[30] with a rate $R_{phot_X} n_X$.

5) Species on the surface can meet and react to form a product that will either stay on the surface or be released into the gas phase[10].

The rate equation method couples the equations describing the different populations of the surface species. These equations are written as:

$$\frac{d(X_i)}{dt} = R_{acc_{X_i}} - X_i X_j \alpha_{X_i} + (1-f_{des})X_j X_k \alpha_{X_j} - R_{evapx_i} X_i - R_{phot_{X_i}} X_i + R_{phot_{X_j}} X_j,\qquad(4)$$

where X_i are the species on the surface. The six terms of this equation represent (1) the accretion of species X_i from the gas phase, (2) the formation of new species that involve species X_i, (3) the creation of species X_i by the encounter of species X_i and X_j that are present on the surface, (4) the evaporation of species X_i, (5) the photo-dissociation of X_i on the dust, and (6) the creation of X_i by photo-dissociation of species Y.

The formation of OH, H_2O and O_2 are insured by several reactions routes on the dust but only the reaction O + H, OH + H and O + O see their products (OH, H_2O and O_2) released in the gas phase. The different gas phase efficiencies due to the chemistry on dust can be written as followed:

$$\epsilon_{OH} = \frac{fdes_{OH} n_O n_H \alpha_H}{k_a cc(O)}\qquad(5)$$

$$\epsilon_{H_2O} = \frac{fdes_{H_2O} n_{OH} n_H \alpha_H}{k_a cc(O)}\qquad(6)$$

$$\epsilon_{O_2} = \frac{2fdes_{O_2} n_O^2 \alpha_O}{k_a cc(O)}\qquad(7)$$

with fdes the chemical desorption fraction for the considered reaction as reported in table 2.

Formation rates on dust due to chemical desorption. The formation rates of species X can be written as: $k_{X,dust} = n_O v_O n_{dust} \sigma \epsilon_X$, where n_{dust} is the density of dust, σ the dust cross section and ϵ_X the efficiency of the formation of OH, H_2O or O_2 (eq. 5, 6 and 7) . If we consider a MRN grain size distribution ($n_{dust}\sigma/n(H) = 10^{-21}$ cm^{-2}), then the rates for the formation of OH, H_2O and O_2 are written as:

$$\begin{aligned} k_{OH,dust} &= 3.9\cdot10^{-17}\sqrt{\frac{T_{gas}}{100}}\epsilon_{OH}(T_{dust})\text{cm}^3\text{s}^{-1} \\ &= 3.9\cdot10^{-17}\sqrt{\frac{T_{gas}}{100}}\frac{0.3}{1+2\cdot10^{21}\frac{nOI}{nHI^2}\exp-\frac{1100}{T_{dust}}}\text{cm}^3\text{s}^{-1} \end{aligned}\qquad(8)$$

$$\begin{aligned} k_{H_2O,dust} &= 3.9\cdot10^{-17}\sqrt{\frac{T_{gas}}{100}}\epsilon_{H_2O}(T_{dust})\text{cm}^3\text{s}^{-1} \\ &= 3.9\cdot10^{-17}\sqrt{\frac{T_{gas}}{100}}\frac{0.7}{1+2\cdot10^{21}\frac{nOI}{nHI^2}\sqrt{\frac{100}{T_{gas}}}\exp-\frac{833}{T_{dust}}}\text{cm}^3\text{s}^{-1} \end{aligned}\qquad(9)$$

$$k_{O_2,dust} = 1.9\cdot10^{-17}\sqrt{\frac{T_{gas}}{100}}\epsilon_{O_2}(T_{dust})\text{cm}^3\text{s}^{-1}\qquad(10)$$

$$= 1.9\cdot10^{-17}\sqrt{\frac{T_{gas}}{100}}\frac{1.3\cdot10^{-23}nOI\sqrt{\frac{T_{gas}}{100}}\cdot\exp\frac{-500}{T_{dust}}}{den^2}$$

$$\text{cm}^3\text{s}^{-1},\qquad(11)$$

where nHI and nOI are the densities of atomic hydrogen and oxygen in the gas phase, respectively. The rate for the formation efficiency of O_2 is complex, and the denominator of the expression (den) is written as:

$$den = 1.5 \cdot 10^{22} \cdot n_{HI} \cdot \sqrt{\frac{T_{gas}}{100}} \cdot \exp\frac{143}{T_{dust}} + \exp\frac{-1076}{T_{dust}} + \exp\frac{-500}{T_{dust}} \cdot OH \quad (12)$$

With OH the approximate of the OH surface species on the dust:

$$OH = \frac{0.26 \frac{nOI}{nHI} \cdot \exp\frac{-143}{T_{dust}}}{1 + \frac{0.6 \cdot 10^{22} \exp\frac{-1343}{T_{dust}}}{nHI\sqrt{\frac{T_{gas}}{100}}}} \quad (13)$$

As the temperature increases, some reactants evaporate and we enter a stochastic regime where the system should be treated with stochastic methods (Monte Carlo). Therefore, the rates we derive here overestimate the actual rates at temperatures greater than 30 K[24] (when the rates decrease exponentially). Note that the value of T_{dust} for the validity of our estimates is higher at higher densities.

Formation rates in the gas phase. In the gas phase, the formation routes of water (OH + H$_2$) and OH (O + H$_2$) are associated with barriers of 1736 K, 3150 K, respectively[25]. These rates can be written as:

$$k_{OH,gas} = 3.14 \cdot 10^{-13} \left(\frac{T_{gas}}{300}\right)^{2.70} \exp\left(-\frac{3150}{T_{gas}}\right) cm^3 s^{-1} \quad (14)$$

$$k_{H_2O,gas} = 2.05 \cdot 10^{-12} \left(\frac{T_{gas}}{300}\right)^{1.52} \exp\left(-\frac{1736}{T_{gas}}\right) cm^3 s^{-1}. \quad (15)$$

1. Trumpler, R. J. Absorption of Light in the Galactic System. *PASP* **42**, 214 (1930).
2. Oort, J. H. & van de Hulst, H. C. Gas and smoke in interstellar space. *Bull. Astron. Inst. Netherlands* **10**, 187 (1946).
3. Walmsley, C., *Interstellar Dust*, Allamandola, L. J. & Tielens, A. G. G. M. eds. (1989), vol. **135** of *IAU Symposium*, 263.
4. Kristensen, L. E. *et al.* Methanol maps of low-mass protostellar systems. I. The Serpens molecular core. *A&A* **516**, A57 (2010).
5. Takahashi, J. & Williams, D. A. Chemically driven desorption of CO from icy grains in dark clouds. *MNRAS* **314**, 273 (2000).
6. Andersson, S., Al-Halabi, A., Kroes, G.-J. & van Dishoeck, E. F. Molecular-dynamics study of photodissociation of water in crystalline and amorphous ices. *Journal of Chemical Physics* **124**, 064715 (2006).
7. Morisset, S., Aguillon, F., Sizun, M. & Sidis, V. Quantum dynamics of H$_2$ formation on a graphite surface through the Langmuir Hinshelwood mechanism. *Journal of Chemical Physics* **121**, 6493 (2004).
8. Bergeron, H., Rougeau, N., Sidis, V., Sizun, M., Teillet-Billy, D. & Aguillon, F. OH Formation from O and H Atoms Physisorbed on a Graphitic Surface through the Langmuir Hinshelwood Mechanism: A Quasi Classical Approach. *Journal Phys. Chem. A* **112**, 11921 (2008).
9. Garrod, R. T., Wakelam, V. & Herbst, E. Non-thermal desorption from interstellar dust grains via exothermic surface reactions. *A&A* **467**, 1103 (2007).
10. Cazaux, S., Cobut, V., Marseille, M., Spaans, M. & Caselli, P. Water formation on bare grains: When the chemistry on dust impacts interstellar gas. *A&A* **522**, A74+ (2010).
11. Pirronello, V., Liu, C., Shen, L. & Vidali, G. Laboratory Synthesis of Molecular Hydrogen on Surfaces of Astrophysical Interest . *ApJL* **475**, L69+ (1997).
12. Pirronello, V., Liu, C., Roser, J. E. & Vidali, G. Measurements of molecular hydrogen formation on carbonaceous grains. *A&A* **344**, 681 (1999).
13. Amiaud, L., Dulieu, F., Baouche, S., Fillion, J. H., Momeni, A. & Lemaire, J. L. Isotopic Segregation of Molecular Hydrogen on Water Ice Surface at Low Temperature: Importance for Interstellar Grain Chemistry. eds. (2006), vol. **855** of *American Institute of Physics Conference Series*, 55–61.
14. Congiu, E., Matar, E., Kristensen, L. E., Dulieu, F. & Lemaire, J. L. Laboratory evidence for the non-detection of excited nascent H$_2$ in dark clouds. *MNRAS* **397**, L96 (2009).
15. Noble, J. A. *et al.* The desorption of H$_2$CO from interstellar grains analogues. *A&A* **543**, A5 (2012).
16. Miyauchi, N., Hidaka, H., Chigai, T., Nagaoka, A., Watanabe, N. & Kouchi, A. Formation of hydrogen peroxide and water from the reaction of cold hydrogen atoms with solid oxygen at 10 K. *Chemical Physics Letters* **456**, 27 (2008).
17. Ioppolo, S., Cuppen, H. M., Romanzin, C., van Dishoeck, E. F. & Linnartz, H. Laboratory Evidence for Efficient Water Formation in Interstellar Ices. *ApJ* **686**, 1474 (2008).
18. Dulieu, F. *et al.* Experimental evidence for water formation on interstellar dust grains by hydrogen and oxygen atoms. *A&A* **512**, A30 (2010).
19. Pettersson, M., Tuominen, S. & Räsänen, M. IR Spectroscopic Study of H$_2$O$_2$, HDO$_2$, and D$_2$O$_2$ Isolated in Ar, Kr, and Xe Matrices. *JPC A* **101** (6), 1166–1171 (1997).
20. Cazaux, S. & Tielens, A. G. G. M. H$_2$ Formation on Grain Surfaces. *ApJ* **604**, 222 (2004).
21. Fraser, H. J., Collings, M. P., McCoustra, M. R. S. & Williams, D. A. Thermal desorption of water ice in the interstellar medium. *MNRAS* **327**, 1165 (2001).
22. Jing, D., He, J., Brucato, J., De Sio, A., Tozzetti, L. & Vidali, G. On Water Formation in the Interstellar Medium: Laboratory Study of the O + D Reaction on Surfaces. *ApJL* **741**, L9 (2011).
23. Congiu, E., Chaabouni, H., Laffon, C., Parent, P., Baouche, S. & Dulieu, F. Efficient surface formation route of interstellar hydroxylamine through NO hydrogenation. I. The submonolayer regime on interstellar relevant substrates. *JCP* **137**, 054713 (2012).
24. Meijerink, R., Cazaux, S. & Spaans, M. Enhanced H$_2$O formation through dust grain chemistry in X-ray exposed environments. *A&A* **537**, A102 (2012).
25. Manion, J. A. *et al.* NIST Chemical Kinetics Database NIST Standard Reference Database 17, Version 7.0 (Web Version), Release 1.4.3. Data version 2008.12, National Institute of Standards and Technology, Gaithersburg, Maryland, 20899 8320. Web address: http://kinetics.nist.gov/ (2008).
26. Goldsmith, P. F. *et al.* Herschel Measurements of Molecular Oxygen in Orion. *ApJ* **737**, 96 (2011).
27. Goldsmith, P. F. *et al.* O$_2$ in Interstellar Molecular Clouds. *ApJL* **539**, L123 (2000).
28. Pagani, L. *et al.* Low upper limits on the O$_2$ abundance from the Odin satellite. *A&A* **402**, L77 (2003).
29. Liseau, R. *et al.* Multi-line detection of O$_2$ toward ρ Ophuichi A. *A&A* **541**, A73 (2012).
30. Cuppen, H. M. & Herbst, E. Simulation of the Formation and Morphology of Ice Mantles on Interstellar Grains. *ApJ* **668**, 294 (2007).

Author contributions
S. Cazaux and F. Dulieu wrote the main manuscript. The experiements were perfomed by E. Congiu, J. A. Noble, S. Baouche, H. Chaabouni, A. Moudens, M. Minissale and F. Dulieu. S. Cazaux developed the theoretical model. All authors reviewed the manuscript.

Additional information

How to cite this article: Dulieu, F. *et al.* How micron-sized dust particles determine the chemistry of our Universe. *Sci. Rep.* **3**, 1338; DOI:10.1038/srep01338 (2013).